B(GT) strength from β-decay measurements and inferred shape mixing in ^{74}Kr

E. Poirier,[1] F. Maréchal,[1] Ph. Dessagne,[1] A. Algora,[2,*] M. J. G. Borge,[3] D. Cano-Ott,[4] J. C. Caspar,[1] S. Courtin,[1] J. Devin,[1] L. M. Fraile,[5,†] W. Gelletly,[6] G. Heitz,[1] A. Jungclaus,[3,7] G. Le Scornet,[5] Ch. Miehé,[1] E. Nácher,[2] B. Rubio,[2] P. Sarriguren,[3] J. L. Tain,[2] O. Tengblad,[3] C. Weber,[1] and the ISOLDE Collaboration[5]

[1]*Institut de Recherches Subatomiques, IN$_2$P$_3$-CNRS, F-67037 Strasbourg, Cedex 2, France*

[2]*Instituto de Física Corpuscular, CSIC University of Valencia, E-46071 Valencia, Spain*

[3]*Instituto de Estructura de la Materia, CSIC, E-28006 Madrid, Spain*

[4]*CIEMAT, Avenida Complutense 22, E-28040 Madrid, Spain*

[5]*ISOLDE, Division EP, CERN, CH-1211 Geneva, Switzerland*

[6]*Department of Physics, University of Surrey, Guildford, GU2 5XH, United Kingdom*

[7]*Departamento de Fisica Theorica, Universidad Autonoma de Madrid, E-28049 Madrid, Spain*

(Received 7 May 2003; published 3 March 2004)

A total absorption spectrometer, dedicated to the study of very short-lived atomic species, has been built and installed at the CERN/ISOLDE mass separator. The β decay of the neutron-deficient ^{74}Kr nucleus has been studied using this new device. The Gamow-Teller strength distribution has been observed over most of the Q_{EC} window, and a total strength of 0.69(3) $g_A^2/4\pi$ has been measured for states with excitation energy below 3 MeV. Shape mixing in the ^{74}Kr ground state is inferred from a comparison of the experimental strength distribution with self-consistent, deformed, quasiparticle-random-phase-approximation calculations.

DOI: 10.1103/PhysRevC.69.034307 PACS number(s): 21.10.Pc, 23.40.Hc, 27.50.+e

I. INTRODUCTION

For many years, β-decay experiments have proved to be a powerful tool to study nuclear systems. Today, they continue to provide a wealth of information about fundamental aspects of the nuclear medium and the weak interaction. Such experiments are often also the first to provide information about the nuclear structure of new isotopes. The β decay in allowed processes is governed by a very simple and well understood operator, namely, $\sigma\cdot\tau$ in the case of a Gamow-Teller decay and τ for a Fermi decay. Thus, a good and complete description of the ground state of the parent nucleus and of the states populated in the daughter nucleus should provide, in principle, a good value for the total strength and of the strength distribution over the full Q_β window. Hence, the measurements of these quantities offer a good probe to test our theoretical models.

The $N=Z$, $A\simeq 75$ region of the nuclear chart is of particular interest in terms of nuclear structure because of the wide variety of nuclear shapes displayed in the region. Competing prolate and oblate deformations are predicted due to several different energy gaps in the shell model potential at $Z,N=34-40$, the signature of such effects being rapid changes in nuclear shape when adding or removing only a few nucleons [1,2]. Furthermore, shape coexistence can occur when neutron and proton shell gaps drive the nucleus towards opposite deformations [3,4]. A typical candidate for such behavior is the neutron-deficient ^{74}Kr isotope which has recently been the subject of several in-beam investigations [5,6]. From these studies, possible shape coexistence in this nucleus was inferred from the measurement of the electric-monopole (E0) transition linking the 0_1^+ ground state to a second 0_2^+ isomeric state.

The decay of ^{74}Kr was last studied by Schmeing *et al.* [7]. They established the decay scheme up to 978 keV based on high resolution γ-γ and β-γ coincidence measurements. The total β^+ and electron capture feeding was determined from the difference between the γ feeding and γ decay of each observed level. Yet, no direct experimental evidence of deformation or shape coexistence for this nucleus, nor for other nuclei in this mass region, has so far been obtained through β-decay measurements.

For nuclei close to the proton drip line, theoretical calculations predict that the Gamow-Teller strength will be concentrated at high excitation energy in the daughter nucleus but will still be accessible through β-decay studies with approximately half of the total strength appearing within the β^+-decay window [8,9]. Furthermore, the Gamow-Teller strength distribution calculated as a function of the excitation energy in the daughter nucleus depends sensitively on the ground state deformation of the parent nucleus [9,10].

Although the Gamow-Teller strength distribution B(GT) carries fundamental information about nuclear structure, its determination is not straightforward and meets difficulties on the experimental side. When germanium detectors are used, their limited high energy detection efficiency, combined with the β-strength fragmentation at high excitation energy, leads to systematic errors in both the total B(GT) and the B(GT) distribution. An alternative method is to use the total absorption technique to extract the complete strength distribution. This method is based on measuring the total energy released in the γ decay of each level populated in the β decay of the parent nucleus, and therefore is sensitive to the β population of the nuclear levels rather than to the individual γ rays. This technique, which dates back to the work of Duke *et al.* [11],

*On leave from Insitute of Nuclear Research, Debrecen, Hungary.

†On leave from Dpto. Física Atómica, Molecular y Nuclear, Faculted de Físicas, Univ. Compultense, E-28080 Madrid, Spain.

has been used recently at the Gesellschaft für Schwerionenforschung (GSI) online mass separator to study the decay of isotopes in the region of the doubly magic nucleus ^{100}Sn [12–15], as well as in the spherical rare earth region [16]. These studies showed that if we are to obtain reliable information on the complete β strength, and hence compare experiment and theory, we require measurements with the total absorption spectrometry technique [16,17]. The advantage of applying the total absorption technique to $N \sim Z$ nuclei was already mentioned in Ref. [18].

We have revisited the β decay of neutron-deficient krypton and strontium isotopes using the total absorption spectrometry technique with the aim of determining the total GT strength and the GT distribution over the whole Q_{EC} energy window. Here we present the results obtained for the ^{74}Kr isotope ($Q_{EC}=3140\pm62$ keV). The experiment was performed using a new total absorption spectrometer specifically designed for the study of very short-lived nuclei, and presently installed at the CERN/ISOLDE mass separator. Data were collected and the Gamow-Teller strength extracted over most of the Q_{EC} window. A comparison of the experimental strength distribution with self-consistent deformed Hartree-Fock (HF) plus quasiparticle-random-phase-approximation (QRPA) calculations is presented.

The paper is organized as follows. Section II is devoted to the experimental procedure used in the ^{74}Kr experiment and Sec. III to the extraction of the strength distribution from the raw data. The results are presented in Sec. IV and the ground state deformation of the neutron-deficient ^{74}Kr isotope is discussed. Our findings are summarized and conclusions are drawn in Sec. V.

II. EXPERIMENT

A new total absorption gamma spectrometer (TAgS) [19] has been designed by a Madrid-Strasbourg-Surrey-Valencia collaboration to study very short-lived nuclei at the CERN/ISOLDE mass separator. The spectrometer consists of a large, cylindrical NaI(Tl) monocrystal (38 cm diameter, 38 cm length) with a 7.5 cm hole drilled perpendicular to the symmetry axis. The detector, called *Lucrecia* and manufactured by *Saint-Gobain Crystals and Detectors*, is viewed by eight 5 in. photomultiplier tubes, type Electron Tubes 9792B. The crystal is encased in a 13 mm thick aluminum cylinder whose thickness is reduced to 11 mm inside the radial hole in order to limit the γ-ray absorption. Good light reflection is provided by a 2 mm thick Al_2O_3 coating on the inner side of the aluminum case. The crystal response stability is monitored by a light emitting diode (LED) triggered by a pulse generator.

Excellent energy resolution is achieved. The resolution of the NaI crystal was as good as 7.1% and 5.4% at 662 keV and 1332 keV, respectively. Experimental total and photopeak efficiencies of 95(8)% and 83(7)%, respectively, were measured at 662 keV with a calibrated ^{137}Cs source. Finally, these overall good detection efficiencies and energy resolutions, combined with a solid angle of 97% of 4π, make the new TAgS spectrometer one of the most powerful total absorption spectrometers.

Radioactive isotopes are implanted in a 55 μm thick aluminized mylar tape that can be moved in order to limit the buildup of daughter activity. The tape transport system [20], functioning under vacuum, routinely operates at a speed of 1.3 m/s and possibly at a higher speed of up to 2.0 m/s. A set of three collimators, placed 950 mm, 975 mm, and 992 mm upstream from the collection point, was used to suppress the beam halo and to define a 6×8 mm^2 beam spot on the mylar tape. In these experimental conditions, a transmission of 30% was achieved for a ^{40}Ar stable beam over the 36 m flight path that separates the high resolution separator (HRS) separator from the end of the new RC3 beamline where the spectrometer is installed. The beamline ends with a telescopic aluminum tube (1.2 mm thick, 68 mm diameter) sealed by a 80 μm kapton window.

In order to disentangle the β^+ and electron capture (EC) components of the decay process, x and γ ray as well as β-particle detectors located close to the collection point are used. A germanium telescope consisting of a 1 cm planar detector backed by a 5 cm thick coaxial crystal is used to detect low energy (8 keV$<E_\gamma<$500 keV) γ rays as well as more energetic γ rays. The telescope covers $\sim$14% of the 4π solid angle. The energy resolution obtained with the planar detector is 0.49 keV at 59.5 keV and 2.1 keV at 1332 keV with the coaxial detector. In order to limit the x-ray absorption, the end cap of the telescope cryostat is made of a thin (0.3 mm) beryllium window. A 2 mm thick plastic (NE102) detector located in front of the germanium telescope and covering 13% of 4π completes the setup and is used to detect the β particles. This setup allows direct γ-ray studies as well as $\gamma-\gamma$ and $\beta-\gamma$ coincidences to be performed. A schematic diagram of the experimental setup is presented in Fig. 1.

To reduce the contribution of the background due to the activity (neutrons and gammas) in the experimental hall, the spectrometer and its ancillary detectors are placed inside an 11 ton shield made of a boron polyethylene (10 cm), lead (5.1 cm), copper (1.5 cm), and aluminum (2 cm) sandwich. Shielding efficiencies of 1.0 and 0.9 were calculated for slow ($E_n\sim1$ eV) and fast ($E_n\sim1$ MeV) neutrons, respectively, using the MCNPX 2.2.3 code [21]. All the experimental evidence seems consistent with this shielding efficiency estimate. The counting rate in the TAgS due to the γ background activity is reduced by a factor of 3.5 down to about 1.0 kHz with the shielding closed. The residual activity mainly comes from the decay of ^{40}K present inside the crystal. The temperature inside the closed shielding is regulated to $\pm0.5\,^\circ$C with an industrial air conditioning system.

The experiment was carried out at the ISOLDE online isotope separator at CERN [22]. The ^{74}Kr ion beam was produced by spallation of a thick (43 g/cm^2) Nb target induced by an intense 1.4 GeV proton beam delivered by the CERN-PSB accelerator. A cooled transfer line connects the target and the plasma ion source from which the ions are extracted in their 1^+ charge state and electrostatically accelerated to 60 keV. The cold transmission line strongly suppresses the contamination of noble gas beams by less volatile isobars (e.g., directly produced bromine). The isobaric contamination was found to be negligible, corresponding to a

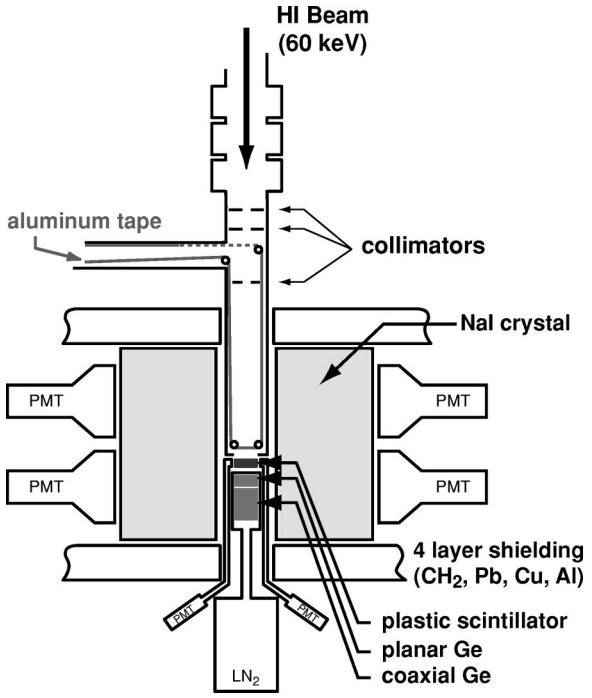

FIG. 1. Schematic diagram of the experimental setup. Heavy ions (HI) are implanted into an aluminized mylar tape in the center of the NaI crystal. All sensitive detectors are placed inside a four layer shielding that reduces the counting rate due to neutron and γ-background activities. Collimators, placed upstream from the collection point, limit the beam spot size on the tape.

suppression factor of more than 10^4, in agreement with previous data collected at $A=72$ and 73 in similar conditions [18,23]. The spallation products were analyzed using the HRS mass separator, and the average production yield for ^{74}Kr was 1.5×10^6 atoms/μC. The mass-separated ^{74}Kr isotopes were collected in the center of the TAgS spectrometer.

A total of 190 measurement cycles, each with a duration of 170 s, was devoted to the experiment on ^{74}Kr, corresponding to a total counting time of 538 min. Due to the high production yield, the target only received one of the 14 proton pulses produced per supercycle, and the ions were collected on the tape for 1.5 s at the beginning of each cycle. At the end of the experiment, another 358 min were devoted to the measurement of the ^{74}Br daughter activity, and a total of 65 min was used to measure the room background.

Data were recorded in two separate modes (direct and coincidence) using conventional electronics in NIM and FERA-based CAMAC standards. Energy signals from the TAgS photomultipliers (eight dynodes) as well as from the plastic detector (two dynodes) and the germanium telescope were recorded using peak-sensing converters. Timing signals between the TAgS and the ancillary detectors were also recorded on tape in the coincidence mode only.

III. ANALYSIS

The quantity we are interested in is the Gamow-Teller strength B(GT) as a function of the excitation energy in the daughter nucleus

$$B(\mathrm{GT}) = \frac{KI_\beta}{f(Q_{EC}-E_x)T_{1/2}}, \tag{1}$$

where I_β is the β branching to a level with E_x excitation energy, $f(Q_{EC}-E_x)$ is the integral of the Fermi function, $T_{1/2}$ is the β-decay half-life in seconds, and $K=3833\pm24$ s [24,25]. Extracting the strength over the full energy range simply relies on the accurate determination of the β branchings to all the states to which the decay can proceed. Although a total absorption spectrometer is sensitive to the β population of the nuclear levels rather than to the individual γ rays, the task is not trivial. The raw experimental spectra must be corrected for the effects of various distortions, one of them being electronic pulse pileup. This effect occurs when two pulses overlap and are interpreted by the analyzing system as corresponding to one real event. Analytic solutions exist to calculate the pileup contribution for quadratic or Gaussian pulse shapes. However, because such solutions remain approximate, we use a numerical pulse pileup correction that requires a knowledge of the true pulse shape. Details of the correction algorithm and method can be found in Ref. [26]. The calculated pileup contribution is then normalized to the experimental spectrum in the energy region beyond the Q_{EC} value. Second and higher order pileup contributions are negligible ($<0.25\%$) if one limits the counting rate to 10 kHz or below.

To obtain the β-decay strength distribution of the parent nucleus from the raw spectra, free of distortion, one must generally also consider and subtract the background and daughter activity contributions. The corrected energy spectra, **d** (counts/channel), can then be related to the level feeding distribution **f** ($\equiv N\,I_\beta$, N=total number of decays) using the equation [27]

$$\mathbf{d} = \mathbf{R}(b)\cdot\mathbf{f}, \tag{2}$$

where $\mathbf{R}(b)$ is the response function matrix of the spectrometer which depends on its characteristics. Each column j of this matrix, called the level j response distribution, also depends on the quanta emitted in the decay, positron for β^+ decay or x ray for EC decay and all the subsequent electromagnetic contributions (γ-ray and/or conversion electron cascades). If one considers that the response to a particle with a given energy does not depend on the response to other particles, then the matrix **R** can be constructed from the individual response distributions through successive convolutions of the adequate single quantum responses [27]. The response function **R** depends also on the γ-branching ratios b in the daughter nucleus, and therefore its computation requires a knowledge of the level scheme in this nucleus. The low energy part of the level scheme is obtained from high-resolution spectroscopy with germanium detectors whereas the unknown upper part is obtained from a decay model of the nucleus. With these assumptions, the TAgS response function was obtained by means of Monte Carlo simulations using the GEANT4 package [28]. The experimental setup geometry was carefully modeled and the light production process in the NaI crystal was included as described in Ref. [27]. Results were compared to experimental data ob-

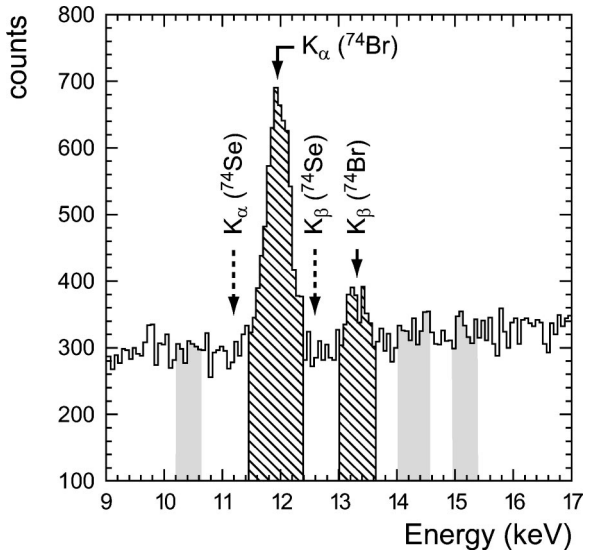

FIG. 2. X-ray spectrum obtained with the germanium planar detector and showing the K_α and K_β transitions in ^{74}Br. The expected positions of the K_α and K_β transitions in ^{74}Se are also shown. The shaded areas show the energy gates used for background subtraction.

tained for different radioactive calibration sources (^{22,24}Na, ^{60}Co, and ^{88}Y). The photon response matrix was then computed for radiations with energies ranging from 20 keV to 8 MeV. The β-response matrix was computed for particles with energies ranging from (Q_β=20 keV to Q_β=2118 keV (i.e., Q_{EC}=3140 keV). Finally, in order to obtain the feeding distribution **f**, Eq. (2) is inverted using the expectation maximization method [29].

By requiring coincidences of TAgS signals with the bromine x rays detected in the germanium planar detector, or with positrons detected in the plastic scintillator, we distinguish between events corresponding to EC or β^+ decay of ^{74}Kr, if one disregards the internal conversion process. However, in the case of β^+ decay, we do not have the detailed knowledge of the plastic detector (e.g., response function to low energy β particles) needed to compute the β efficiencies with high enough accuracy to obtain reliable feedings. Moreover, the strength at high excitation energy in ^{74}Br is not seen due to the 1022 keV energy fraction always missed in β^+ decay and to the relatively high β detection threshold ($E_{\rm cut}$ $\sim$300 keV) cutting off the contribution of low energy β particles. In addition, the existence of a $4^{(-)}$ isomeric state in ^{74}Br with a 41.5 min half-life [30] and an excitation energy of 13.8 keV [31], complicates any subtraction of the daughter activity as the collection-measurement cycles used in the krypton and bromine measurements are different. Therefore, we have limited our analysis to the EC component of the decay by requiring coincidences between the TAgS spectrometer and the x-ray detector.

IV. RESULTS

The x-ray spectrum from the germanium planar detector is shown in Fig. 2. The EC component of the ^{74}Kr decay was

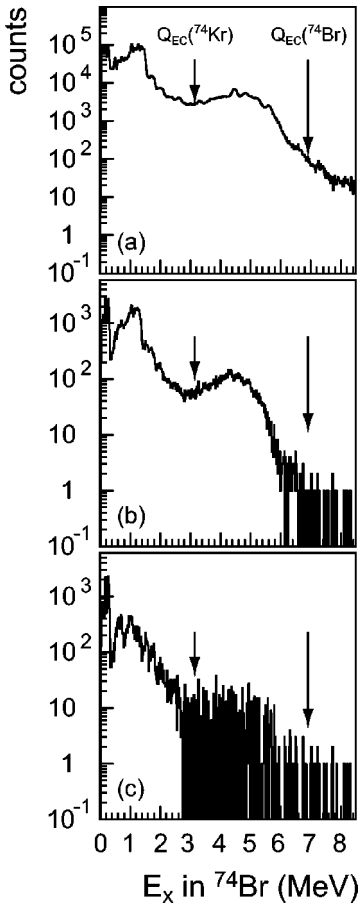

FIG. 3. (a) Direct TAgS spectrum. (b) TAgS spectrum in coincidence with the Br K_α and K_β transitions in the planar detector. (c) Final background subtracted TAgS spectrum corresponding to the EC component of the ^{74}Kr decay. Arrows indicate the ^{74}Kr and ^{74}Br Q_{EC} values.

selected by putting gates on the K_α and K_β transitions in Br located at 11.9 keV and 13.4 keV, as shown in the figure. The resulting spectrum is displayed in Fig. 3(b) and can be compared to the direct TAgS spectrum shown in Fig. 3(a).

The coincidence requirement between the TAgS spectrometer and the x-ray detector reduces the ^{74}Br daughter activity contribution. Nevertheless, undesired coincidences with background signals underneath the x rays, mainly due to the Compton effect or due to the penetration of the β particles into the planar detector, are still possible and must be taken into account. This can be done by subtracting the TAgS contribution in coincidence with the background in the planar detector (shaded areas in Fig. 2) from the spectrum displayed in Fig. 3(b). The final background subtracted EC spectrum is displayed in Fig. 3(c). The contents of the spectrum are combined in 20 keV bins in order to match properly the binning of the calculated response function for further analysis (see Sec. III). The very low statistics beyond the Q_{EC}(^{74}Br) value (6907$\pm$15 keV) in Fig. 3(b) suggest that the electronic pulse pileup contribution was negligible and therefore was not taken into account in the analysis.

The observed statistics in the final spectrum [Fig. 3(c)] between the two Q_{EC} values (^{74}Kr and ^{74}Br) is only due to

TABLE I. β-branching ratios and B(GT) values in units of $g_A^2/4\pi$ for the ^{74}Br levels as determined in this work and compared to previous values from Ref. [7].

E_x (keV)	$I_\beta+I_{EC}$ [7]	$I_\beta+I_{EC}$	B(GT) [7]	B(GT)
0.0	<10	0.0	$<1.0\times10^{-2}$	
9.9		0.0		
72.6		0.0		
89.7	9.6	2.4(2)	11×10^{-2}	$2.8(4)\times10^{-3}$
132.6	0.7	0.0	8.8×10^{-4}	
179.1	1.3	0.020(2)	1.8×10^{-3}	$2.8(4)\times10^{-5}$
212.9	33.6	20(2)	4.9×10^{-2}	$2.9(4)\times10^{-2}$
239.4	1.1	5.8(5)	1.7×10^{-3}	$8.9(1)\times10^{-3}$
306.6	43.4	46(4)	7.8×10^{-2}	$8.3(1)\times10^{-2}$
390.1	0.3	0.06(1)	7.0×10^{-5}	$1.4(2)\times10^{-5}$
534.5	0.9	0.68(6)	2.6×10^{-3}	$2.0(3)\times10^{-3}$
609.1	3.0	3.7(3)	1.0×10^{-2}	$1.3(2)\times10^{-2}$
613.0	0.3		1.0×10^{-3}	
701.3	3.6	5.4(5)	1.6×10^{-2}	$2.4(4)\times10^{-2}$
831.9	0.4	1.1(1)	2.5×10^{-3}	$6.8(1)\times10^{-3}$
970.1	1.0	3.4(3)	8.3×10^{-3}	$2.8(5)\times10^{-2}$
978.0	0.5		4.2×10^{-3}	
978–3000	–	11.4(3)	–	$4.9(3)\times10^{-1}$
total	100	100	1.9×10^{-1}	$6.9(3)\times10^{-1}$

fluctuations coming from the background subtraction. It is estimated to account for only 3% of the initial number of counts in this energy range before subtraction. Because the decay of the $4^{(-)}$ isomeric state in ^{74}Br ($T_{1/2}=41.5$ min) is not favored by our collection-measurement cycle (see Sec. II), and according to the decay scheme of ^{74}Br [7], one expects most of the daughter activity ($\sim$80%) to be located above 3 MeV, the EC spectrum is more than 99% free of background contribution up to Q_{EC} (^{74}Kr).

One should note that the x-ray–TAgS coincidence is not exclusively EC as events corresponding to the β^+ decay of ^{74}Kr can also be selected when the decay is followed by the electron conversion of low energy transitions deexciting levels in ^{74}Br. From the ^{74}Br level scheme [7], and assuming different multipolarities (M1 and E2) for the most intense low energy transitions (62.8 and 89.7 keV), one can estimate the intensity of the internal conversion process following either a EC or β^+ decay. We found that it amounts to 1.3 and 4.8% of the total decay intensity, yielding an upper limit of 8% for the contribution of the β^+ process to the x-ray-gated TAgS spectrum [Fig. 3(c)]. This contamination, spread over the whole Q_{EC} energy window, was not taken into account in the analysis but was included as a systematic error in the final B(GT) values.

To determine the β feedings (see Sec. III), we have considered the level scheme of ^{74}Br established by Schmeing *et al.* [7] for energies up to 978 keV. We have also taken into account the two 1013.8 and 1060.9 keV γ transitions that were identified in Ref. [7] but not placed in the level scheme. In the present work, it was considered that these two transitions were deexciting levels located at these energies. The upper part of the level scheme ($E_x \geqslant 1$ MeV) was derived from the statistical nuclear model. The back-shifted Fermi gas formula [32,33] was used to generate positive and negative parity states with spins $J=0$, 1, and 2, yielding possible E1, M1, E2, and M2 γ transitions in the daughter nucleus. For each transition, the γ width was calculated using the corrected Weisskopf formula [34]. Only allowed GT transitions to 1^+ states in ^{74}Br ($\Delta J=1$, and no parity change) were considered for the β decay. Based on results obtained for neutron-deficient isotopes in the $A=75$ mass region [35,36], the density parameter a was initially chosen to be 10 MeV^{-1}. It was then increased to 11 MeV^{-1} to reproduce the data after better use of the direct relationship given by Eq. (2). Higher values for a do not significantly improve the results as, in that case, the mean energy level spacing becomes smaller than the 20 keV binning of the data. The back-shifted ground state position Δ was fixed at -1.36 MeV [33].

The resulting β feedings are presented in Table I for energies up to 978 keV. Despite the relatively poor energy resolution of NaI crystals, the analysis method allows us to extract the feedings with enough accuracy for a comparison with the values originally obtained by Schmeing *et al.* [7]. Although both results are similar, discrepancies occur due to the different methods. Our feedings are normalized to one over the whole Q_{EC} window, not including the ^{74}Br ground state, whereas feedings from Ref. [7] are normalized over the first 978 keV. Feedings to levels above 1 MeV, not listed in the table, vary from 0.01 to 2% up to 3140 keV. Our experimental method does not allow us to determine the feeding to the ground level of ^{74}Br as no information is available in the spectra. However, because this level has spin and parity 0^- or 1^-, such feeding would primarily come from a first-

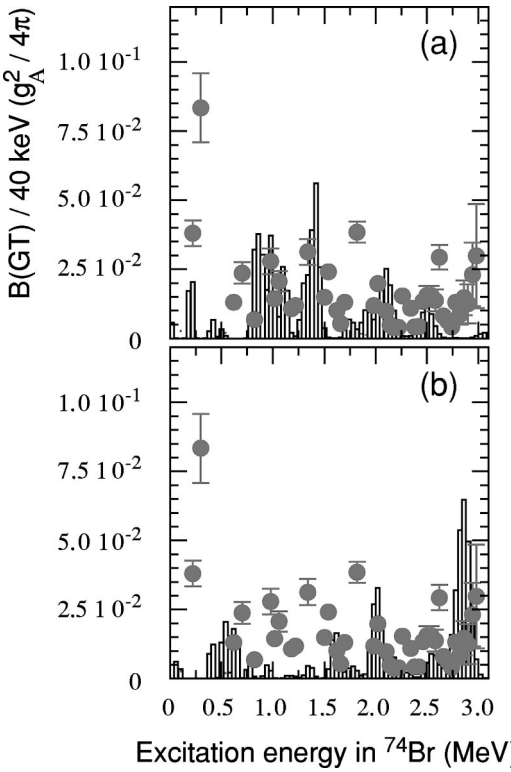

FIG. 4. Experimental Gamow-Teller strength distribution measured for ^{74}Kr (filled circles) compared to self-consistent HF calculations [39,41] assuming for the ^{74}Kr ground state (a) an oblate ($\beta_0 = -0.15$) shape, and (b) a prolate ($\beta_0 = +0.39$) shape. The calculations were performed using the SG2 Skyrme interaction.

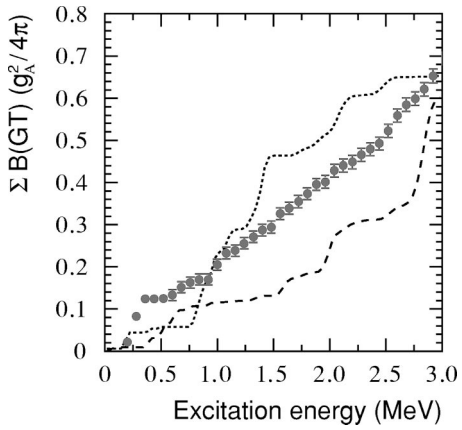

FIG. 5. Accumulated GT strength in ^{74}Kr as a function of the excitation energy of the daughter nucleus. The dotted and dashed lines correspond to the oblate and prolate solutions of HF calculations using the SG2 interaction, respectively.

forbidden, Fermi or Gamow-Teller, transition which is not very likely to occur. Therefore, this feeding has not been taken into account and we have restricted our analysis to allowed Gamow-Teller transitions.

From the β feedings and using the Fermi functions f_0 in Eq. (1), the B(GT) strength was calculated for each transition connecting the ground state of ^{74}Kr to levels in ^{74}Br. Figure 4 presents the experimental B(GT) strength. Mostly due to the uncertainty in the Q_{EC} value (3140±62 keV), we present our results only up to 3 MeV. The total Gamow-Teller strength to states within this energy window is measured to be $0.69(3) g_A^2/4\pi$ (see Table I). The error bars on Fig. 4 include the error in the Q_{EC} value that enters into the calculation of the f_0 Fermi function in Eq. (1). The uncertainty in the ^{74}Kr half-life in the B(GT) calculation, as well as the errors on the feedings coming from the covariance matrices obtained as a result of the analysis method [37] are also taken into account. The resulting B(GT) values to levels with excitation energies up to 978 keV are given in Table I and compared to the values from Ref. [7].

The experimental results in Fig. 4 are compared to calculations based on a deformed HF mean field obtained with the density-dependent SG2 Skyrme force including pairing correlations in the BCS approximation. A residual spin-isospin force is introduced consistently and treated in the QRPA. Details of the calculations can be found in Refs. [38,39]. The calculated GT strength distributions presented in Fig. 4 have been obtained for the two nuclear shapes, oblate ($\beta_0 = -0.15$) and prolate ($\beta_0 = 0.39$), that minimize the HF energy. The strengths are given in units of $g_A^2/4\pi$ and are scaled by a factor 0.6 to account for the quenching of the strength [40] as deduced for this mass region from charge exchange reactions and β-decay measurements. The theoretical results have been folded with Gaussian functions whose widths are given by the experimental resolution of the spectrometer. The resulting strength was then accumulated in 40 keV bins, the same as for the data.

Figure 4 shows that neither of the two calculated GT strength distributions, from pure oblate or prolate shape, can reproduce the experimental B(GT) values over the full range of excitation energy. While the oblate calculation [Fig. 4(a)] reproduces the strength distribution below 2.0 MeV of excitation energy, the prolate calculation [Fig. 4(b)] agrees better with the concentration found at higher energies. In that sense the two pictures complement each other. The same conclusion is obtained from Fig. 5 where we show the experimental accumulated GT strength compared to the results of the HF calculations [39,41]. Again, the experimental data lie systematically in between the two calculations indicating a possible shape mixing in the ground state of ^{74}Kr. Results obtained with other Skyrme forces like Sk3 are qualitatively similar [38].

This result corroborates the most recent Hartree-Fock-Bogoliubov calculations predicting a strong mixture of prolate and oblate shapes in the ground state of ^{74}Kr [42]. It is also consistent with the recent work by Becker *et al.* [6] that concludes that there is 50:50 mixing between coexisting oblate and prolate shapes in this nucleus. Thus, the present work brings an additional and independent experimental confirmation of the ground state shape mixing in ^{74}Kr following numerous in-beam experiments (see Refs. [5,6] and references therein).

V. CONCLUSIONS

A new TAgS spectrometer has recently been successfully used to study the neutron-deficient Kr and Sr isotopes at ISOLDE/CERN. The experimental Gamow-Teller B(GT) strength of ^{74}Kr has been measured for the first time over most of the Q_{EC} window. A total strength of 0.69(3) $g_A^2/4\pi$ has been measured for states with excitation energy up to 3 MeV. Comparisons of the data with HF-BCS-QRPA calculations from 0 to 3 MeV indicate a possible shape mixing in the ground state of ^{74}Kr which is found to be neither oblate nor prolate.

For the first time, information on the nuclear shape of unstable nuclei in the $A=75$ mass region has been inferred from β-decay studies. Although this method is model dependent, it opens new possibilities for probing the nuclear structure of other nuclei provided that one undertakes the necessary theoretical developments to extract unambiguous results from our strength distribution measurements in the case of shape mixing.

ACKNOWLEDGMENTS

The authors would like to thank their colleagues, engineers, and technicians, from the IReS-Strasbourg and CLRC-Daresbury, whose collaboration has been so valuable during the development of the TAgS project and during the first experiment. The collaboration is especially grateful to M. de Saint Simon from the CSNSM-Orsay for providing us with the beam transport calculations for the new ISOLDE RC3 beamline. This work has been partly supported by EPSRC (UK), by the IN_2P_3/CNRS (France) and CICYT (Spain) under Contract Nos. PN98-1 and PN00-1, by the CICYT under Contract No. AEN99-1046-CO2-01/02, by the MCyT under Contract No. BFM2002-03562, and by the European Large Scale Facility Grant No. HPRI-CT-1999-00018. A. Algora is a post-doctoral research fellow under the Marie Curie Contract No. HPMF-CT-1999-00394. A. Jungclaus acknowledges financial support from the Deutsche Forschungsgemeinschaft (DFG) within the Heisenberg program.

[1] W. Nazarewicz, J. Dudek, R. Bengtsson, T. Bengtsson, and I. Ragnarsson, Nucl. Phys. **A435**, 397 (1985).
[2] P. Bonche, H. Flocard, P. H. Heenen, S. J. Krieger, and M. S. Weiss, Nucl. Phys. **A443**, 39 (1985).
[3] P. H. Heenen, P. Bonche, J. Dobaczewski, and H. Flocard, Nucl. Phys. **A561**, 367 (1993).
[4] A. Petrovici, K. W. Schmid, and A. Faessler, Nucl. Phys. **A605**, 290 (1996).
[5] C. Chandler, P. H. Regan, C. J. Pearson, B. Blank, A. M. Bruce, W. N. Catford, N. Curtis, S. Czajkowski, W. Gelletly, R. Grzywacz, Z. Janas, M. Lewitowicz, C. Marchand, N. A. Orr, R. D. Page, A. Petrovici, A. T. Reed, M. G. Saint-Laurent, S. M. Vincent, R. Wadsworth, D. D. Warner, and J. S. Winfield, Phys. Rev. C **56**, R2924 (1997).
[6] F. Becker, W. Korten, F. Hannachi, P. Paris, N. Buforn, C. Chandler, M. Houry, H. Hübel, A. Jansen, Y. Le Coz, C. F. Liang, A. Lopez-Martens, R. Lucas, E. Mergel, P. H. Regan, G. Schönwasser, and Ch. Theisen, Eur. Phys. J. A **4**, 103 (1999).
[7] H. Schmeing, J. C. Hardy, R. L. Graham, and J. S. Geiger, Nucl. Phys. **A242**, 232 (1975).
[8] I. Hamamoto and H. Sagawa, Phys. Rev. C **48**, R960 (1993).
[9] I. Hamamoto and X. Z. Zhang, Z. Phys. A **353**, 145 (1995).
[10] F. Frisk, I. Hamamoto, and X. Z. Zhang, Phys. Rev. C **52**, 2468 (1995).
[11] C. L. Duke, P. G. Hansen, O. B. Nielsen, G. Rudstam, and ISOLDE Collaboration, Nucl. Phys. **A151**, 609 (1970).
[12] M. Karny, L. Batist, B. A. Brown, D. Cano-Ott, R. Collatz, A. Gadea, R. Grzywacz, A. Guglielmetti, M. Hellström, Z. Hu, Z. Janas, R. Kirchner, F. Moroz, A. Piechaczek, A. Plochocki, E. Roeckl, B. Rubio, K. Rykaczewski, M. Shibata, J. Szerypo, J. L. Tain, V. Wittmann, and A. Wöhr, Nucl. Phys. **A640**, 3 (1998).
[13] M. Karny, L. Batist, B. A. Brown, D. Cano-Ott, R. Collatz, A. Gadea, R. Grzywacz, A. Guglielmetti, M. Hellström, Z. Hu, Z. Janas, R. Kirchner, F. Moroz, A. Piechaczek, A. Plochocki, E. Roeckl, B. Rubio, K. Rykaczewski, M. Shibata, J. Szerypo, J. L. Tain, V. Wittmann, and A. Wöhr, Nucl. Phys. **A690**, 367 (2001).
[14] Z. Hu, L. Batist, J. Agramunt, A. Algora, B. A. Brown, D. Cano-Ott, R. Collatz, A. Gadea, M. Gierlik, M. Górska, H. Grawe, M. Hellström, Z. Janas, M. Karny, R. Kirchner, F. Moroz, A. Plochocki, M. Rejmund, E. Roeckl, B. Rubio, M. Shibata, J. Szerypo, J. L. Tain, and V. Wittmann, Phys. Rev. C **60**, 024315 (1999).
[15] Z. Hu, L. Batist, J. Agramunt, A. Algora, B. A. Brown, D. Cano-Ott, R. Collatz, A. Gadea, M. Gierlik, M. Górska, H. Grawe, M. Hellström, Z. Janas, M. Karny, R. Kirchner, F. Moroz, A. Plochocki, M. Rejmund, E. Roeckl, B. Rubio, M. Shibata, J. Szerypo, J. L. Tain, and V. Wittmann, Phys. Rev. C **62**, 064315 (2000).
[16] J. Agramunt, A. Algora, D. Cano-Ott, A. Gadea, B. Rubio, J. L. Tain, M. Gierlik, M. Karny, Z. Janas, A. Plochocki, K. Rykaczewski, J. Szerypo, R. Collatz, J. Gerl, M. Górska, H. Grawe, M. Hellström, Z. Hu, R. Kirchner, M. Rejmund, E. Roeckl, M. Shibata, L. Batist, F. Moroz, V. Wittmann, and P. Kleinheinz, in *Proceedings of the SGR97 on New Facet of Spin Giant Resonances in Nuclei, Tokyo, Japan, 1997*, edited by H. Sakai, H. Okamura, and T. Wakasa (World Scientific, Singapore, 1998), p. 150.
[17] A. Algora, D. Cano-Ott, B. Rubio, J. L. Tain, J. Agramunt, J. Blomqvist, L. Batist, R. Borcea, R. Collatz, A. Gadea, J. Gerl, M. Gierlik, M. Górska, O. Guilbaud, H. Grawe, M. Hellström, Z. Hu, Z. Janas, M. Karny, R. Kirchner, P. Kleinheinz, W. Liu, T. Martinez, F. Moroz, A. Plochocki, M. Rejmund, E. Roeckl, K. Rykaczewski, M. Shibata, J. Szerypo, and V. Wittmann, Nucl. Phys. **A654**, 727c (1999).
[18] Ch. Miehé, Ph. Dessagne, Ch. Pujol, G. Walter, B. Jonson, M. Lindroos, and the ISOLDE Collaboration, Eur. Phys. J. A **5**, 143 (1999).

[19] E. Poirier, Ph.D. thesis, Université de Strasbourg 2002; Internal Report No. IReS-03-01.
[20] R. Dissert, H. Friedmann, M. Klipfel, A. Krauth, R. Limbach, and G. Walter, CRN Internal Report ISSN 0775-3404, 1990.
[21] H. G. Hughes, R. E. Prael, and R. C. Little, MCNPX - The LAHET/MCNP Code Merger, X-Division Research Note XTM-Rn(U)97-012, Los Alamos National Laboratory Report No. LA-UR-97-4891 1997.
[22] E. Kugler, Hyperfine Interact. **129**, 23 (2000).
[23] I. Piqueras, M. J.G. Borge, Ph. Dessagne, J. Giovinazzo, A. Huck, A. Jokinen, A. Knipper, C. Longour, G. Marguier, M. Ramdhane, V. Rauch, O. Tengblad, G. Walter, Ch. Miehé, and the ISOLDE Collaboration, Eur. Phys. J. A **16**, 313 (2003).
[24] I. S. Towner, E. Hagberg, J. C. Hardy, V. T. Koslowsky, and G. Savard, in *Proceedings of the ENAM95 Exotic Nuclei and Atomic Masses, Arles, France*, 1995, edited by M. de Saint Simon and O. Sorlin (Editions Frontières, Gif-sur-Yvette, 1995), p. 711.
[25] K. Schreckenbach, P. Liaud, R. Kossakowski, H. Nastoll, A. Bussiere, and J. P. Guillaud, Phys. Lett. B **349**, 427 (1995).
[26] D. Cano-Ott, J. L. Tain, A. Gadea, B. Rubio, L. Batist, M. Karny, and E. Roeckl, Nucl. Instrum. Methods Phys. Res. A **430**, 488 (1999).
[27] D. Cano-Ott, J. L. Tain, A. Gadea, B. Rubio, L. Batist, M. Karny, and E. Roeckl, Nucl. Instrum. Methods Phys. Res. A **430**, 333 (1999).
[28] S. Agostinelli *et al.*, Nucl. Instrum. Methods Phys. Res. A **506**, 250 (2003).
[29] A. P. Dempster, N. M. Laird, and D. B. Rubin, J. R. Stat. Soc. Ser. B. Methodol. **39**, 1 (1977).
[30] A. Coban, J. C. Lisle, G. Murray, and J. C. Willmott, Part. Nuclei **4**, 108 (1972).
[31] J. Döring, J. W. Holcomb, T. D. Johnson, M. A. Riley, S. L. Tabor, P. C. Womble, and G. Winter, Phys. Rev. C **47**, 2560 (1993).
[32] E. Erba, U. Facchini, and E. Saetta-Menichella, Nuovo Cimento **22**, 1237 (1961).
[33] W. Dilg, W. Schantl, H. Vonach, and M. Uhl, Nucl. Phys. **A217**, 269 (1973).
[34] P. M. Endt, At. Data Nucl. Data Tables **23**, 547 (1979).
[35] Ch. Miehé, J. Giovinazzo, Ph. Dessagne, A. Huck, A. Knipper, G. Marguier, C. Longour, V. Rauch, M. J.G. Borge, I. Piqueras, O. Tengblad, A. Jokinen, M. Ramdhane, and ISOLDE Collaboration, in ENAM98, Exotic Nuclei and Atomic Masses, edited by Bradley M. Sherrill, David J. Morrissey, and Cary N. Davids, AIP Conf. Proc. No. 455 (AIP, Woodbury, 1998), p. 789.
[36] J. Giovinazzo, Ph. Dessagne, and Ch. Miehé, Nucl. Phys. **A674**, 394 (2000).
[37] D. Cano-Ott, Ph.D. thesis, University of Valencia, 2000.
[38] P. Sarriguren, E. Moya de Guerra, A. Escuderos, and A. C. Carrizo, Nucl. Phys. **A635**, 55 (1998).
[39] P. Sarriguren, E. Moya de Guerra, and A. Escuderos, Nucl. Phys. **A658**, 13 (1999).
[40] G. Martínez-Pinedo, A. Poves, E. Caurier, and A. P. Zuker, Phys. Rev. C **53**, R2602 (1996).
[41] P. Sarriguren, E. Moya de Guerra, and A. Escuderos, Nucl. Phys. **A691**, 631 (2001).
[42] A. Petrovici, K. W. Schmid, and A. Faessler, Nucl. Phys. **A665**, 333 (2000).